Coastal Engineering 90 (2014) 85–94

Contents lists available at ScienceDirect

Coastal Engineering

journal homepage: www.elsevier.com/locate/coastaleng

A parametric model for barred equilibrium beach profiles

Robert A. Holman [a,*], David M. Lalejini [a], Kacey Edwards [b], Jay Veeramony [b]

[a] Marine Geosciences Division, Naval Research Laboratory, Code 7440.3, Bldg 1005, Stennis Space Center, MS 39529-5004, USA
[b] Oceanography Division, 1009 Balch Blvd, Naval Research Laboratory, Stennis Space Center, MS 39529, USA

ARTICLE INFO

Article history:
Received 24 October 2013
Received in revised form 18 March 2014
Accepted 19 March 2014
Available online 10 May 2014

Keywords:
Bathymetry estimation
Remote sensing
Nearshore
Equilibrium beach
Parametric profiles

ABSTRACT

Environment predictions for locations for which bathymetric data is missing, poor or outdated requires the use of some sort of representative bathymetric form, usually one that is concave up but monotonic. We propose and test a parametric form that superimposes realistic sand bars (Ruessink et al., 2003b) on a background profile that mixes a concave up nearshore with a planar far field behavior. Implementation at any new site involves estimation of five parameters, three that can be found from approximate information from climatology or old offshore charts, one that can be estimated by almost any remote sensing modality and one, h_{sea} that is less well understood but mostly affects deeper bathymetry that has little impact on the resulting surf zone hydrodynamics. Tests against several hundred surveys at three diverse locations show that bathymetry is better estimated by the new barred form than with a previous monotonic profiles in about 80% of cases. The remaining cases are usually associated with the parametric prediction of bars that look realistic but are out of phase. The presence of parametric bars has an even greater impact on predicted hydrodynamics since wave breaking is concentrated at sand bar locations. Modeled cross-shore transects of alongshore current and wave height over the measured survey profile are well represented by modeled transects over the barred parametric form but not for results over a Dean profile. The peak alongshore current strength and location are particularly sensitive to the presence of a sand bar.

Published by Elsevier B.V.

1. Introduction

A primary goal of research in the nearshore zone (defined here as the region where waves are significantly affected by the bottom) is to predict the hydrodynamics and morphodynamics driven by waves propagating over sandy beaches. Response depends strongly on the pre-existing bathymetry, a variable that can be measured only with great effort and that changes rapidly on time scales that range from days to weeks under wave and storm forcing, to decades and centuries under changing climate and sea level. Given the impracticality of measuring or predicting these changes over time, there is a clear need to develop parametric forms for bathymetry that approximate the important features of beach form as it affects hydrodynamics. The most common class of assumed parametric forms is equilibrium beach profiles (EBP), technically the asymptotic shape approached by a beach profile under constant forcing, but other climatologically-representative forms could also be used as long as they represent typical (preferred) forms under natural forcing.

Equilibrium beach profile forms have been studied extensively as a most plausible proxy for cases of unknown or poorly known bathymetry and also for long-term applications such as beach response to sea level rise (see Özkan-Haller and Brundidge (2007) for a recent review). Ideally, the shape of an EBP is found from an assumed depth-dependent sediment transport equation by finding the profile shape for which the transport is equal to zero everywhere, for example as done by Bowen (1980). However, they are more commonly just simple parametric forms with desirable characteristics such as being concave upward.

The best known EBP form is the power law approach first proposed by Bruun (1954) but commonly referred to as the Dean profile due to his extensive field investigations into the problem (e.g. Dean, 1991)

$$h = Ax^{2/3} \tag{1}$$

Here h is depth, x is cross-shore distance from the shoreline and A is a dimensional constant that was found to depend on an assumed uniform sediment grain size (see, for example, Dean, 1987). This form was empirical but motivated by the concept that transport should redistribute sediment such that the breaking dissipation per unit volume will be constant. This model has the advantage of simplicity, has only one parameter that can be determined, in principle, from local site information, and represents the expected concave-up form typically found on wave-dominated beaches. However, the slope at the shoreline is infinite, a problem in some calculations, and decreases continually offshore making it hard to match the typical planar continental shelf outside the nearshore wave zone. Thus the model is typically applied only over a limited cross-shore span.

* Corresponding author. Tel.: +1 541 737 2914.
E-mail addresses: holman@coas.oregonstate.edu (R.A. Holman), David.Lalejini@nrlssc.navy.mil (D.M. Lalejini), kacey.edwards@nrlssc.navy.mil (K. Edwards), jay.veeramony@nrlssc.navy.mil (J. Veeramony).

http://dx.doi.org/10.1016/j.coastaleng.2014.03.005
0378-3839/Published by Elsevier B.V.

Several alternate forms have been proposed to deal with the shoreline singularity. Larson and Kraus (1989) suggested a form that superimposed a planar shallow water component with an offshore Dean form. Özkan-Haller and Brundidge (2007) suggested a modification to further limit the influence of the planar component to shallow water. Bodge (1992) and Komar and McDougal (1994) suggested an exponential form as a preferred solution that exhibited finite slope at the shoreline and a desired concave up profile. However, profiles unrealistically flattened to a horizontal surface offshore.

The solutions discussed above capture desirable characteristics for long-term average profile shape so they can be useful for investigations of long-term sediment volume response, for example, to rising sea level. However, they cannot represent the near-ubiquitous presence of sand bars. Since wave dissipation is focused over bars, hydrodynamic predictions such as nearshore circulation or peak wave height made using beach profiles that omit these features will have little value.

Ruessink et al. (2003b; hereafter RWHKvE03) investigated the possibility of representing barred profiles by analyzing extensive data sets from six beaches around the world and developing a general equation (described in the section below) that represented sand bars in terms of a sinusoidal function with spatially varying amplitude and wavelength. This bar function, h_{bar}, is superimposed on an underlying background bathymetry, h_0, that might be derived from long-term average data or from one of the EBP equations noted above. Thus the total bathymetry would be

$$h(x,t) = h_0(x) + h_{bar}(h_0,t) \tag{2}$$

where we have assumed only a cross-shore dependence (alongshore variability would be represented by implementing Eq. (2) in an alongshore variable way). Because the bar function is formulated in terms of depth, the selected h_0 must be a reasonable representation of the time-mean bathymetry at the site.

The purpose of this paper is two-fold. The first is to introduce a new EBP form that satisfies the requirements of a) finite shoreline slope, b) a concave up form in wave-dominated shallow waters, and c) an asymptotic planar slope in the far field. The second is to develop and test methods to apply the combined bathymetry model (Eq. (2), combining the new background EBP model with the barred model of RWHKvE03) at any site, where the main required input for any realization is a single bar location estimate such as can be determined from wave breaking patterns detected in remote sensing images.

The next section describes the new EBP model and the methods for superimposing the Ruessink model with minimal inputs. This is followed by a section testing the resulting bathymetry predictions using data from three natural beaches and a section comparing hydrodynamic predictions using parametric profiles with those from measured profiles. Thereafter follow discussion and conclusions.

2. EBP profile model

2.1. EBP background profile model

We require a parametric background profile that is concave near the shore but asymptotes to a planar form offshore, mimicking the transition from shapes that are associated with waves versus geological shelf processes. We propose a mix of a planar form with an exponential shoreward component,

$$h_0 = \alpha + \beta + \gamma\exp(-kx) \tag{3}$$

and refer to this as a composite profile. As for the Dean Eq. (1), we assume a shore-based coordinate system so $h = 0$ at $x = 0$ and Eq. (3) can be re-written

$$h_0 = \gamma[\exp(-kx) - 1] + \beta x. \tag{4}$$

Here β, γ and k are three unknown empirical coefficients. Thus, three boundary conditions are needed.

It will be assumed that the value for β, the asymptotic offshore beach slope, can be estimated independently from charts or other information to be β_0. Similarly, we will assume that depth, h', is known at some location, x' (which can be anywhere on the profile but should be representative of the background, average, profile depth so should best be a point seaward of the active sand bar zone). Thus,

$$hx' = \gamma\left[\exp\left(-kx'\right) - 1\right] + \beta_0 x'. \tag{5}$$

The third boundary equation could also be based on another known depth but it is likely that any shoreward point that could help constrain the exponential part of the profile will be influenced by temporally varying sand bars. Instead, the final boundary condition was solved by assuming that the shoreline beach slope was known or could be easily determined. Taking the derivative of Eq. (4) to find slope

$$\frac{dh_0}{dx} = -\gamma k\exp(-kx) + \beta_0. \tag{6}$$

If the shoreline slope is β_s, we have

$$\beta_s = -\gamma k + \beta_0. \tag{7}$$

Note that β_s must be an estimated climatological slope, not an instantaneous fluctuating value. Eqs. (5) and (7) can be solved simultaneously (numerically) to find k and γ. If the profile is convex up (β_0 intersects the shoreline above $z = 0$) the solution is imaginary and a plane slope is substituted from x' to the shoreline.

Fig. 1 shows an example comparison between the Dean and composite background profiles along with an example bathymetry from Duck, NC, on September 16, 2009. The addition of the exponential term allows more profile curvature close to the shoreline and corrects a Dean profile problem of under-predicting shallow water depths. Since the bar profile, described below, depends on depth, this change is important to nearshore bar parameterization. Note that nearshore curvature can also be better estimated by using different exponents in

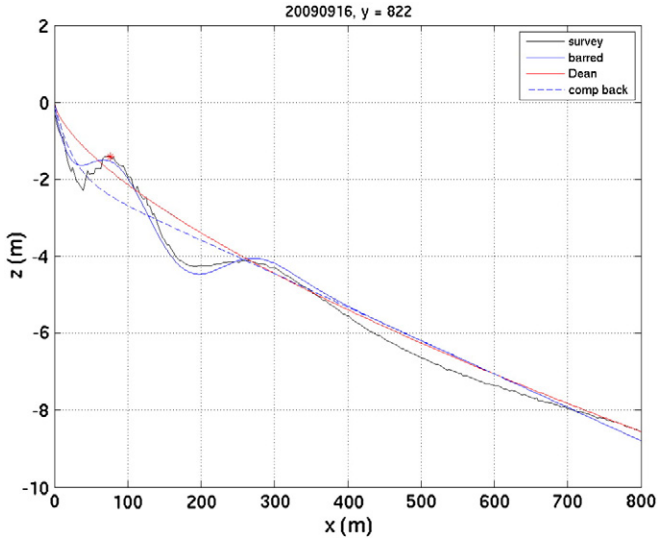

Fig. 1. Comparison of the Dean (red solid), the composite (blue dashed) background profile and the parametric barred profile (solid blue; discussed below) with an example CRAB survey transect (black solid) from Duck, NC, Sept 16, 2009 ($y = 822$ m). Neither background form is capable of representing the sand bars although the composite profile has a much lower bias, especially near the shore. The red asterisk indicates the automatically selected x_b for this profile, discussed below.

Eq. (1), but offshore slopes become correspondingly flattened and the Dean form is typically unable to represent both nearshore and offshore slopes.

2.2. Bar profile model

RWHKvE03 proposed a depth-dependent parametric form for natural sand bars

$$h_{bar}(h_0, t) = -S(h_0)R(t)\cos[\theta(h_0) - \psi(t)] \tag{8}$$

where $S(h_0)$ and $R(t)$ are the spatial and temporal variability of the sand bar profile envelope and the bar function is of a cosine form. The argument of the cosine includes $\theta(h_0)$ that determines the spatial bar lengths (not the envelope of bar amplitude) and $\psi(t)$ that determines temporal changes in bar location. RWHKvE03 then used extensive survey data from six beaches in three countries to develop analytical forms for S, R and θ.

They found that bar amplitude changes over time were small (i.e. bars change position much more than they grow or decay), so R(t) was set to 1.0 (this agrees with early observations by Plant et al. (2001)). The spatial envelope of bar amplitude was well modeled by a skewed Gaussian of the form

$$S = \delta + (S_{max} - \delta)\exp\left[\frac{-\left\{\left(1 - \frac{h_0 - h_{shore}}{h_{sea} - h_{shore}}\right)^a - b\right\}^2}{c}\right]. \tag{9}$$

Instead of being an explicit function of x, it depends on the background (mean) depth, h_0, everywhere in the transect (a function of x). The maximum size of the Gaussian is given by S_{max} and the bar amplitudes are only considered significant if they exceed a noise floor threshold of δ, taken empirically as 0.3. h_{shore} and h_{sea} are the landward and seaward limits of significant bar activity (amplitude > δ). a, b and c are found empirically to be 0.53, 0.57 and 0.09 respectively and it was determined that

$$S_{max} = 0.2h_{sea}. \tag{10}$$

No universal values were found for h_{shore} and h_{sea} so site-specific values were found by least squares fit to data sets for each site.

RWHKvE03 limited their parametric model data fitting to only the regions of significant sand bar signal (S > δ), neglecting regions landward of h_{shore} and seaward h_{sea}. For forward model applications discussed herein where noise is not an issue, bathymetric profiles must be predicted over all depths, so implementation choices must be made for $S(h_0)$ in these domains. An exponential decay was invoked seaward of h_{sea}, matching the slope and value at that location to determine coefficients. For the landward region ($h < h_{shore}$), we require that h = 0 at the shoreline, x = 0 (shore-based coordinate system) and that S = δ at $h = h_{shore}$, so we replace the constant offset, δ, in Eq. (9) with a linear ramp. We must adjust S_{max} accordingly so that $S = S_{max}$ at the appropriate location. The resulting modified form is

$$S = \delta\frac{x}{x_{off}} + \left(S_{max} - \delta\frac{x_{max}}{x_{off}}\right)\exp\left[\frac{-\left\{\left(1 - \frac{h_0 - h_{shore}}{h_{sea} - h_{shore}}\right)^a - b\right\}^2}{c}\right] \tag{11}$$

where x_{max} is the x location at which the exponential function is a maximum. We recognize that these adjustments to allow predictions at both ends of the profile are ad hoc, but feel that they are sensible.

While S describes the amplitude of bars as a function of depth, the cosine term, $\cos[\theta(h_0) - \psi(t)]$, models the actual sand bar form. If we compare to a typical spatial form $\cos(2\pi x/L) = \cos(kx)$, we see that the local wavenumber, k (equal to 2π/L where L is the local bar wavelength), can be found everywhere as the gradient of phase (dθ / dx). Inversely, the required phase structure can be found as

$$\theta(x) = \int_{x_{off}}^{x} \frac{2\pi}{L(x)}\,dx \tag{12}$$

where the integral starts from the offshore limit of the domain and proceeds inward to every x, using the depth, h_0, at each x location. Bar wavelengths are found to be surprisingly well predicted by an empirical relationship

$$L(h_0) = a_L \exp(b_L h_0(x)) \tag{13}$$

where best fit values of a_L and b_L are found to be 100 and 0.27, respectively (Ruessink et al., 2003b).

The only remaining unknown, and the only variable to be measured in order to model the bar at any time, is the temporal phase, ψ(t). Examining Eq. (8), we see that bar crests (defined as the minimum depths of the bar function) will occur when the argument of the cosine equals zero. Thus, if we can independently identify a bar position, x_b, we can find

$$\psi(t) = \theta(x_b) \tag{14}$$

where θ was found using Eq. (10). With this, all the components of Eq. (8) are known and the bar function for any background profile was determined. Summing the background profile with the bar function (Eq. (2)) yields a beach profile that we refer to as a "barred profile" whose fit to example measured bathymetries will be tested below.

The equations above make use of twelve parameters, three for the background profile (β, γ and k, assuming a shore-based coordinate system) and nine for the bar function (h_{sea}, h_{shore}, δ, a, b, c, a_L, b_L and x_b). By comparison, the Dean profile (Eq. (1)), which can only be directly compared to composite background profile, appears to require only one parameter although it really represents two degrees of freedom, A, and the exponent of x which has been empirically fit to the 2/3 value. Thus, it appears that most of the apparent complexity lies in the bar function. In fact, six parameters are considered universal and are known by the six-beach calibrations from the original Ruessink et al., 2003a paper (δ, a, b, c, a_L, b_L), two are site dependent ((h_{sea}, h_{shore}) and one (x_b) varies in time so they must be determined for any realization. It was also determined that the value of h_{shore}, the landward limit of significant bar activity that was required for the Ruessink EOF analysis of noisy data, could safely be set to 0.0 without harming forward model predictions. Table 1 lists the required parameters and how values were selected.

Table 1
List of parameters for parametric model as well as values or methods for determining their values. The first four values require regional knowledge, for example from charts while the fifth value (bar position) must be determined by the user, for example from the location of breaking over a sand bar as seen by remote sensing imagery. The final seven parameters were derived in a six-beach calibration in RWHKvE03.

Parameter	Value
β_0	Offshore slope from chart data
γ	Numerical solution based on single offshore depth and shoreline slope
k	
h_{sea}	Site knowledge
x_b	User selected bar location
h_{shore}	0.0
δ	0.3
a	0.53
b	0.57
c	0.09
a_L	100.0
b_L	0.27

3. Field data tests

The above parametric barred beach forms were compared against measured bathymetry data collected from three U.S. field sites, Duck, North Carolina, beaches from U.S. Pacific Northwest (PNW; southern Washington and northern Oregon), and Eglin Air Force Base (AFB), Florida. The objective was to compare the ability of the composite barred profile to fit natural observations with that of the simpler Dean form and also to determine the relative merits of hydrodynamic predictions made using each parametric form.

For typical applications, the bar crest position, x_b, would be determined from breaking patterns in remote sensing imagery as has been done for years with Argus video imagery (e.g. Lippmann and Holman, 1989; van Enckevort and Ruessink, 2001). However, for the current tests against ground truth surveys, the additional link to imagery was extraneous, and it was decided to estimate x_b directly from the survey data as the location of maximum deviation between the survey data (smoothed with a loess filter with 20 m smoothing scale) and the estimated composite profile. To make the process more robust, the largest absolute deviation was found over the range of candidate depths (out to h_{sea}) and set to a bar for positive deviations ($\theta(x) - \psi(t) = 0$) or a trough for negative deviations ($\theta(x) - \psi(t) = \pi$). Note that only a single x_b position was found per survey profile and the entire cross-shore barred profile (potentially multiple bars and troughs) than predicted using Eqs. (8) and (2).

For the Dean profile, the value of A was found by forcing the curve through the offshore point [x_{sea}, h_{sea}], the same point used to constrain the composite profile, that represents offshore data that could be extracted from a chart for poorly known locations.

Several measures were used to compare parametric models with ground truth data. Bias and root mean square (rms) error are traditional and easy to interpret measures. However, the measurement of sand bar variability can be more difficult since a well-predicted bar shape that is spatially misplaced can give a larger rms bathymetry error than a monotonic beach form that predicts no bars at all. However, since hydrodynamics depend strongly on bathymetric gradients, for example, through gradients of radiation stress, the presence of this non-monotonic variability is vital to good hydrodynamics predictions. In other words, if bathymetry is represented in terms of wavenumber spectra, the hydrodynamic impact of bar features increases with an increase in wavenumber up to bathymetric wavelengths that are shorter than the incident waves. To assess the spectral representation of nearshore bathymetry, we compute the Fourier transform of the detrended nearshore bathymetry and compare the magnitude of the first six spatial Fourier coefficients of parametric versus surveyed bathymetry. The results are presented in terms of the regression slope, m, of parametric versus surveyed Fourier coefficients with a value of 1.0 being a perfect slope, and the R^2 of the fit. In all cases we compare statistics from parametric barred profiles with those of unbarred (composite and Dean) profiles. We recognize that unbarred profiles make no pretense of representing bars, so the comparison is unfair, but we still use the unbarred statistics as a comparison baseline.

In a later section of this paper, the importance of proper representation of bar-scale features on resulting hydrodynamics will be reinforced by comparing modeled hydrodynamic variables over surveyed, parametric barred and parametric unbarred profiles.

All performance measures were computed from the shoreline to h_{sea}, the active volume of sand bar variability.

3.1. Duck, NC, example

Tests were carried out using 15 CRAB surveys collected between May 2009 and August 2011 at Duck, NC, roughly one every two months. Each survey consisted of 26 profiles, all of which had roughly 3.5 m sampling and spanned to at least 8 m depth, roughly 600 m from shore. Tests have shown the vertical accuracy of CRAB surveys to be 5 cm (Birkemeier and Mason, 1984). The presence of the FRF pier at the middle of the research property has been found to introduce severe bathymetry anomalies (e.g. Plant et al., 1999) so the region within 200 m of the pier was excluded from analyses (as was also done in Ruessink et al., 2003a), leaving 18 profiles.

Since many profiles were available, required climatological input parameters were found from the data. For each survey and each alongshore profile, the shoreline location, x_s, and offshore location, x_{sea}, were found as the cross-shore locations where $h = 0$ and $h = h_{sea}$, respectively. The value of β_s was found as the mean slope in the vertical range of ± 0.5 m around x_s while the offshore slope, β_{sea}, was taken as the mean slope between x_{sea} and the seaward limit of the survey. Values for the 15 surveys were averaged to yield climatological values.

Fig. 1 shows an example barred parametric profile. The rms and bias errors between the barred and surveyed profiles were 0.19 and 0.02 m, considerably better than predictions from unbarred Dean (0.59 and −0.37 m) and composite (0.53 and −0.04 m) forms discussed above (see Table 2 for a summary of all performance statistics). The composite form has considerably lower bias than the Dean result. This represents a quite good example prediction, within the upper 5th percentile in rms error and 10th percentile in bias. For comparison, Fig. 2 shows a typical example (rms error–global rms error of 0.48 m). The bar structure is well represented but the outer bar/trough is incorrectly located. Still, the rms and bias between the barred model and survey were 0.45 and −0.12 m, respectively, better than that of just the composite profile (0.58 and −0.18 m) or the Dean profile (0.77 and −0.59 m). Presumably, the parametric bars would be important to predicted hydrodynamics (discussed below).

The multiple surveys and longshore locations allowed 253 comparisons (31 were unusable due to missing profiles or short survey transects) including many that showed bar morphologies that were not well represented by the climatological Ruessink et al. form. Nevertheless, for 78% of the comparisons, the rms fit was improved using the barred parametric form with composite background compared to the Dean equation while the bias was improved in 97% of the cases. Similarly, the composite profile alone improved the rms and bias in 87% and 97% of the cases over the Dean profile. The global rms and bias errors associated with the various parametric forms are listed in Table 2 and show the parametric barred profile to have the lowest error. Cases where the barred profile was worse than the simpler Dean profiles, despite a lack of bars in the latter, were primarily caused by the predicted and surveyed bars being out of phase. Since one of the bar crest locations was correctly located by definition, since it was a model input, the misplacement of other bars can only occur if the wavelength function, Eq. (13), was inappropriate for that particular survey. The reason for this occasional deviation is not known.

Duck profiles usually exhibit one dominant bar with a more subdued second bar offshore, so the Fourier (spectral) representation of bathymetry was dominated by the first few Fourier coefficients. Not surprisingly, in 93% of cases the spectral shape of nearshore bathymetry was better represented by the parametric barred form than the monotonic Dean profile. The best fit regression slope (Table 2) between the first six parametric and surveyed Fourier magnitudes averaged 0.68 ($R^2 = 0.61$), much closer to the ideal 1.0 than the mean slope when comparing the Dean background profile and survey Fourier magnitudes (0.25).

3.2. The role of h_{sea}

The main unknown climatological parameter is h_{sea}, defined by RWHKvE03 as the seaward limit of significant bar activity ($S > \delta$). The selection of h_{sea} has two consequences; it defines the seaward limit of the bar envelope and it also determines the maximum amplitude, S_{max}, of the bars (Eq. (10)). In addition, in this paper, the fit statistics are also calculated over depths from 0 to h_{sea}, introducing an analysis sensitivity. Like h_{shore}, the criterion for choosing the value of h_{sea} as a

Table 2
Summary of fit statistics between parametric (barred, unbarred composite and Dean) and surveyed bathymetry for each of the three beaches. rms and bias errors (meters) are measured from the shoreline to h_{sea}. m and R^2 are the best-fit slope and R^2 for the fit between parametric and survey spectral coefficient magnitudes (ideal is m = 1 and R^2 = 1). Three values of h_{sea} were tested for Eglin AFB. Composite and Dean surveys were tested only for h_{sea} = 8.0 m.

Beach	Barred-survey				Composite-survey				Dean-survey			
	rms	bias	m	R^2	rms	bias	m	R^2	rms	bias	m	R^2
Duck, NC	0.45	0.02	0.68	0.61	0.47	−0.01	–	–	0.60	−0.35	0.25	0.57
PNW	0.95	−0.30	0.91	0.54	1.12	−0.27	–	–	1.13	−0.20	0.25	0.70
Eglin AFB												
h_{sea} = 6 m	0.62	0.42	0.93	0.92								
h_{sea} = 8 m	0.71	0.48	1.24	0.93	1.04	0.74			0.93	0.65	0.31	0.20
h_{sea} = 10 m	0.85	0.58	1.43	0.85								

threshold for separating signal from noise in data may be less applicable to the current case of forward modeling parametric profiles in the absence of noise. Thus a range of possible values were investigated. Fig. 3 shows example barred profiles for a variety of h_{sea} values, illustrating this sensitivity.

RWHKvE03 found that h_{sea} = 3.9 provided the best fit to noisy data at Duck, NC. Table 3 compares the fit statistics using four different test values of h_{sea}. We conclude that a higher value gives a better combination of rms and bias error and have used h_{sea} = 4.5 for best performance. This is about 15% larger than the published value.

3.3. Pacific Northwest examples

Cross-shore profiles were supplied by the Nearshore Morphology Monitoring group at Oregon State University for three beaches in the Columbia River region of the Pacific Northwest. 6 profiles were from Clatsop Plains, Oregon, just south of the Columbia River, 24 were from Long Beach, Washington, just north of the Columbia, and 8 were from Grayland Beach, north of the Columbia between Willipa Bay and Grays Harbor. All data were collected by combining jet ski fathometer data (boat position determined by RTK GPS) with subaerial topography collected using RTK-GPS mounted on an ATV (Ruggiero et al., 2005, 2007). The overall system vertical accuracy is approximately 0.15 m (Ruggiero, pers. comm.). All data were collected between July 28 and August 24, 2010, in the late summer during times of shoreward accretion.

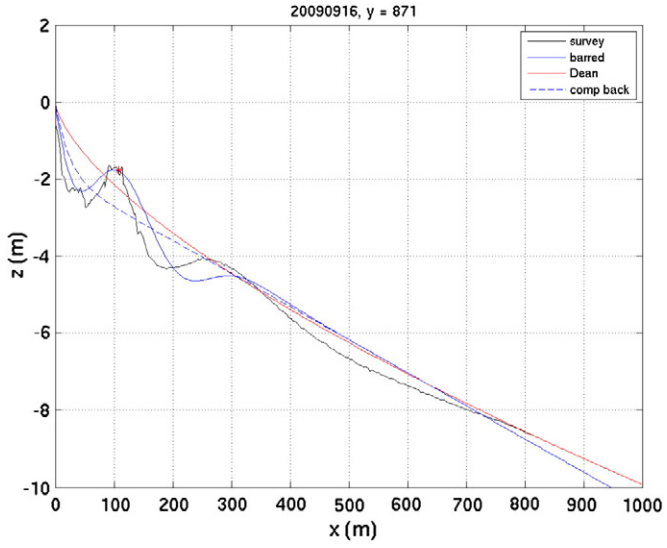

Fig. 2. Second example profile comparing the data (black solid) with the parametric barred profile (solid blue) for Sept 16, 2009, y = 871 m. This example was chosen for having average performance statistics (rms error 0.45 m, bias −0.12 m). The dashed blue line indicates the background composite profile, the red solid line the Dean profile and the red asterisk the automatically selected bar crest location, x_b.

Required parameters were determined from the data as follows. Shoreline and offshore locations, x_s and x_{sea} were determined from individual profiles, mimicking the determination of x_s from a remote sensing source and x_{sea} from charts as some reasonable contour seaward of the sand bar zone. h_{sea} was visually determined as a reasonable seaward limit of bar activity and varied by beach (6.0 m Clatsop, 6.0 Grayland and 9.0 Long Beach). β_s was estimated as a climatological value for each beach and was found as the alongshore average of the mean shoreline slopes over the mean tide range (z = 1.0 ± 1.5 m). Similarly, β_{sea} was the alongshore-average for each beach of the slope between x_{sea} and the seaward limit of survey data. One sand bar location, x_b, for each profile was determined as the location of a local maximum in the deviation profile (survey data minus composite background profile) within the sand bar region.

Fig. 4 shows two example surveys from Grayland Beach along with composite and Dean background profiles and the parametric barred profile. For both cases (and always), a single selected bar location (red asterisk) determines the phase of the entire cross-shore bar profile (three bars in this case). The upper panel (line 68) is a good example for which the barred parametric profile matches the observed locations for all three bars. rms and bias errors are lower for the barred parametric profile (0.52, −0.21 m, respectively) than for the unbarred composite (0.60, −0.15) or Dean (0.68, −0.26) profiles, although the difference is smaller than might be expected based on the visual match. The lower panel (line 48) also looks visually plausible but is statistically a poor fit because the bar wavelengths are not well modeled by equilibrium scales so the inner bars are out of phase with the surveyed bars and the rms error is actually larger (0.74 m) than for the unbarred parametric forms (0.66 m for both composite and Dean background profiles).

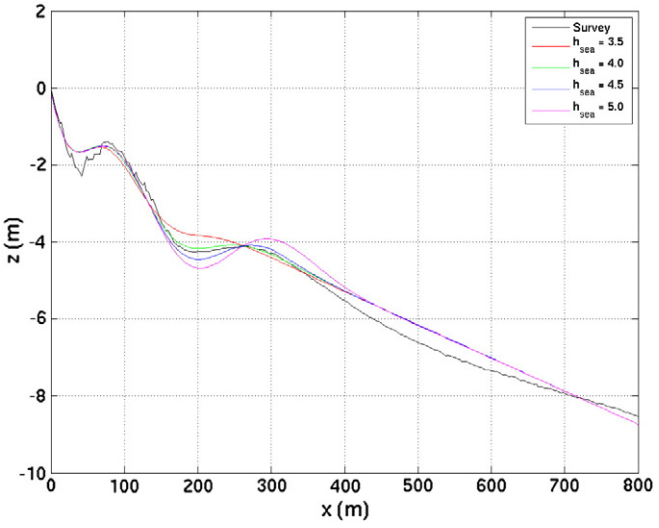

Fig. 3. Comparison of the survey data (black solid line) with predicted barred profiles for various values of h_{sea} (see legend). Increasing h_{sea} both extends the bar envelope to seaward and increases the maximum amplitude.

Table 3
Bulk performance statistics for the different parametric models (barred, composite unbarred and Dean). The last two columns compare the fit statistics of the Dean profile to that of both the barred and composite unbarred profiles, simply counting the percentage of profiles for which each out-performed the Dean profile fit in rms and bias statistics.

Hsea	Barred rms (bias)	Composite rms (bias)	Dean rms (bias)	Barred % better rms/bias	Composite % better rms/bias
3.5	0.43 (0.12)	0.61 (0.24)	0.61 (−0.15)	83/79	49/77
4.0	0.44 (0.02)	0.57 (0.08)	0.63 (−0.30)	81/87	69/87
4.5	0.45 (0.02)	0.47 (−0.01)	0.61 (−0.37)	78/97	89/97
5.0	0.55 (0.21)	0.48 (0.17)	0.55 (−0.26)	57/96	70/96

Computing the statistics for all PNW profile comparisons confirms the above phase shift issues of multiple-barred beaches (Table 2). Of the 38 profiles tested, the rms statistics were improved for 28 (73%) of the barred parametric profiles over the monotonic Dean profile, although the average level of improvement was only 10%. Interestingly, the improvement was beach dependent with only 50% improvement for the 14 profiles of Clatsop and Grayland beaches but 87% of the 24 Long Beach profiles. The potential importance to these statistics of late summer bar disequilibrium will be discussed later. In addition, the bias for the parametric barred profiles were roughly comparable or slightly worse (−0.30 m average) than that for the Dean monotonic profile (−0.20) indicating the sensitivity of the bathymetry-only comparisons to predicting bars that are out of phase with ground truth. The consequences of the inclusion of bars to predicted hydrodynamics will be explored in the next section.

Spectral comparisons were much more clear and measure the presence of variability at sand bar wavelengths rather than the correct phase (Table 2). In comparing the magnitudes of the first six Fourier terms (scales representing from one to six bars in the active bar zone) for surveyed data versus the parametric barred profile, the regression slopes averaged 0.91 ± 0.22 (1 std), much closer to the ideal 1.0 than the regression slope between the Dean background profile and surveyed bathymetry (mean slope 0.25 ± 0.07). The mean R^2 of the parametric barred regressions was 0.54. Thus the parametric barred form does a good job representing the bathymetric variability at the sand bar scale for these beaches.

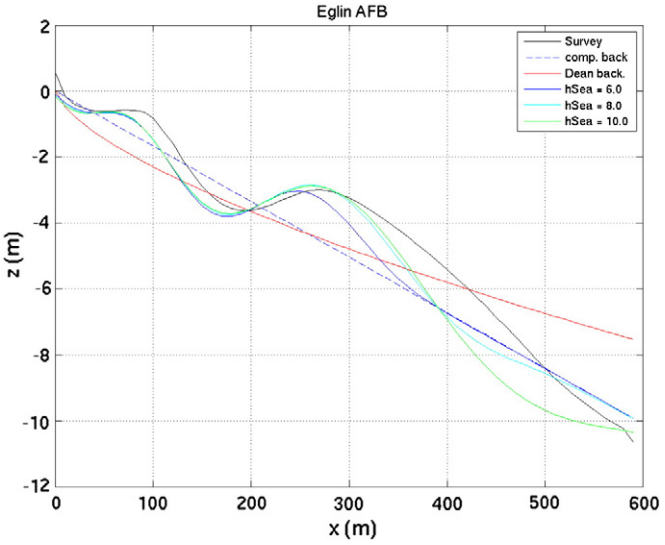

Fig. 5. Bathymetry for Eglin AFB, showing survey data (black), composite (blue dashed) and Dean (red) background profiles as well as barred parametric profiles based on three different values of h_{sea}.

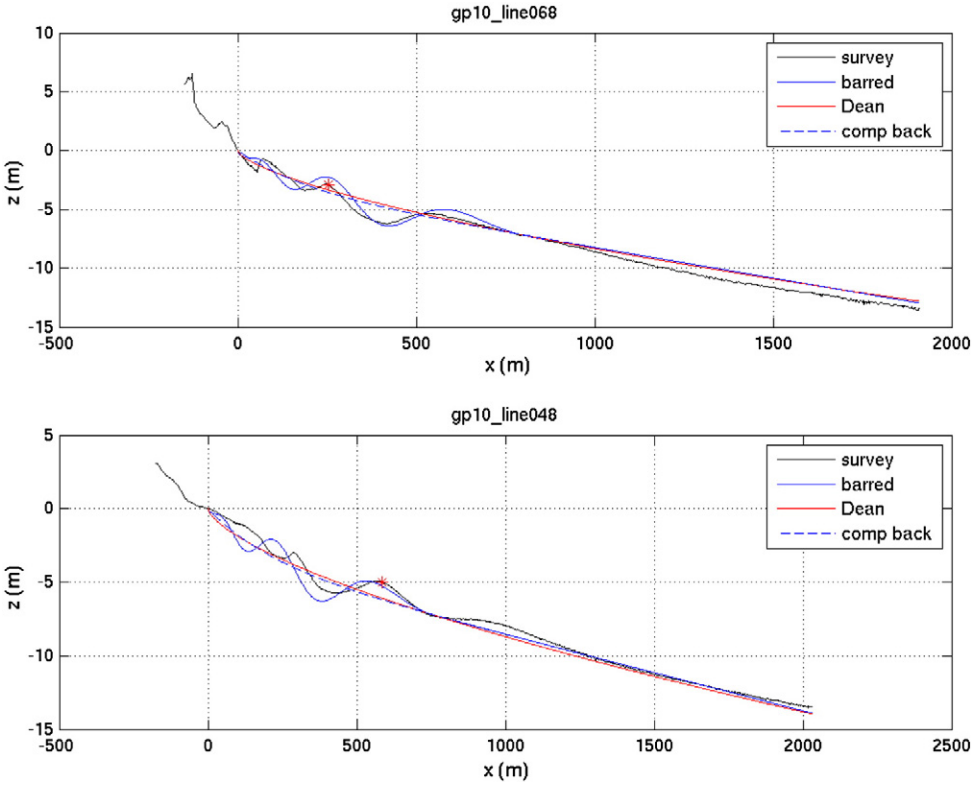

Fig. 4. Comparison of surveyed bathymetry (black) with parametric barred predictions (blue solid) and composite (blue dashed) and Dean (red) monotonic background profiles. The red asterisk marks the bar position used to set the cross-shore phase of the bar.

3.4. Eglin AFB

The final data set came from Eglin Air Force Base, at Fort Walton, Florida, on the Gulf of Mexico. Data were collected in January 2009, using a jet ski system similar to that described above. Initial data were smoothed by loess interpolation to a 10 × 10 m grid spanning 600 m in the across-shore and longshore directions and rotated to a shore-normal coordinate system. The data were then alongshore-averaged to yield a single cross-shore profile which showed two sand bars (Fig. 5).

As before, the shoreline location is assumed to be observable so was taken from the data. Similarly, an offshore point was taken from the data at x = 500 m, mimicking the idea of extracting a contour from a nautical chart or similar source. Shoreline and offshore beach slopes were found using the same approach as for the PNW beaches. Unlike the other sites, the Eglin profile featured a convex-up background profile so the composite background was automatically replaced by a linear slope from the offshore to the shoreline contours. The value of x_b, the sand bar location, was manually chosen as 280 m, corresponding to the crest of the outer bar. There is little environmentally-based guidance for the value of h_{sea}, the seaward depth limit of the active bar zone. Ruessink et al. (2003b) list best fit values for six beaches that average 5.96 m excluding the anomalously low value for Duck. However the observed profile shows bars out to at least 10 m depth (Fig. 5). Thus, parametric barred profiles were produced for test values of h_{sea} of 6.0, 8.0 and 10.0 m (Fig. 5).

In all the three cases, the fit to survey data is visually very good (Table 2). rms (and bias) errors for the parametric barred profiles for these cases were 0.62 (0.42), 0.71 (0.48) and 0.85 (0.58) m, respectively, certainly improved over the 0.93 (0.65) m rms (and bias) error for

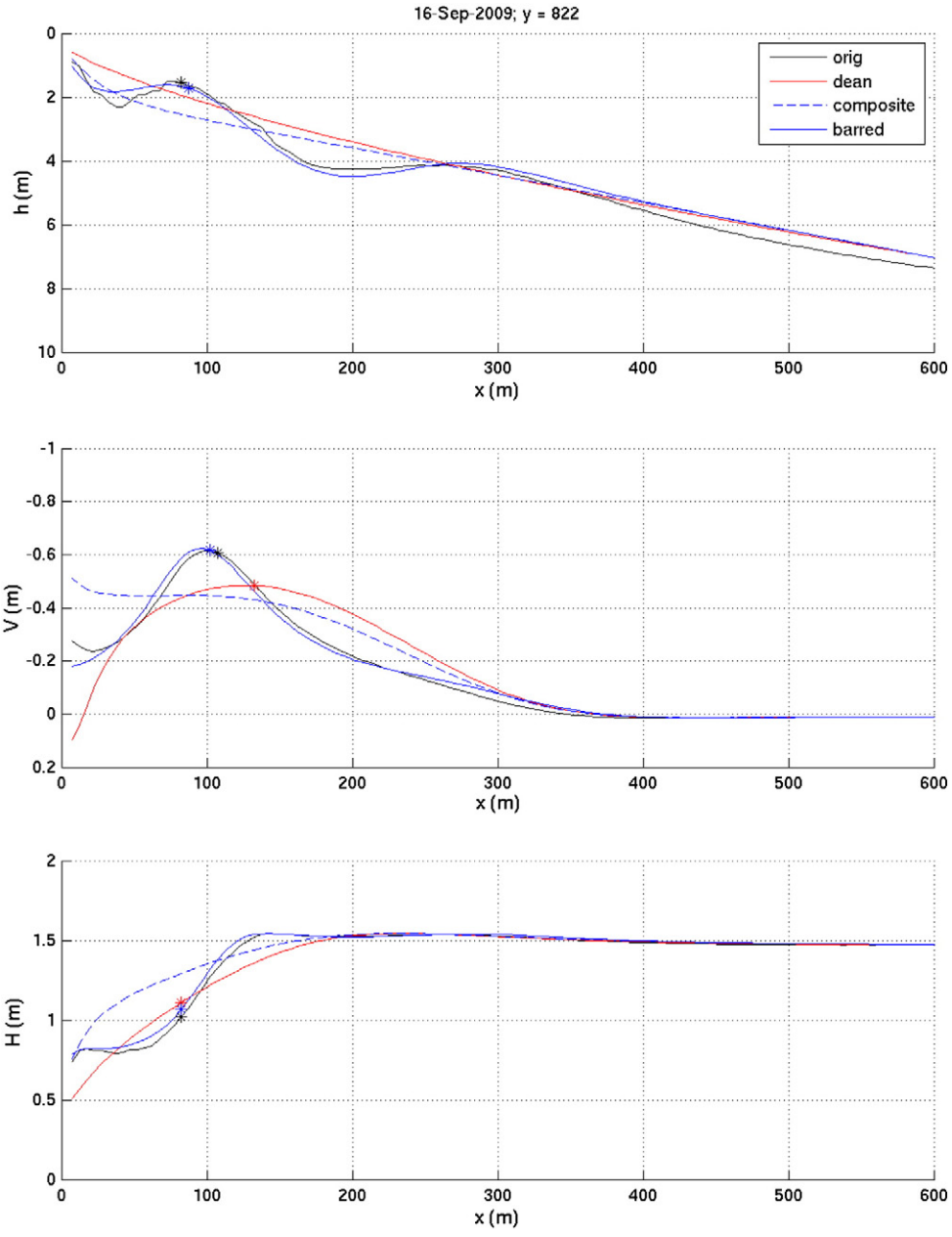

Fig. 6. Cross-shore profiles of bathymetry (upper panel), longshore current (middle panel) and significant wave height (bottom panel) computed for the true and parameterized bathymetries. Current and wave height decay for the barred profile is a much better approximation of truth than the broad current and slow wave height decay predicted for the unbarred parametric models. Asterisks indicate the locations of maximum bar deviation from the background profile (top panel), of maximum current (middle panel), and wave height values at the ground truth bar location (bottom panel).

the Dean profile. Comparisons of the magnitudes of the first six Fourier coefficients between parametric and survey data form for the three values of h_{sea} showed best fit slopes (0.92, 1.24 and 1.43) that were much closer to the ideal slope of 1.0 than the Dean profile slope of (0.31). R^2 values of all fits were high.

A secondary effect of changing h_{sea} is its effect on the attenuation of the offshore bar and consequently the offshore bar crest location. Since crest location is defined in terms of the cosine in the bar function, it may not completely correspond to the location of minimum total depth, h. This issue is lessened if inner bar locations are chosen in shallower water.

4. Hydrodynamic modeling

While a simplified representation of bathymetry is valuable on its own, the largest benefit of improved bathymetry is the associated improvements to hydrodynamic predictions. As is evident below, cross-shore profiles of wave height and longshore currents computed for a monotonic beach profile look very different from those on a barred profile where breaking is strongly concentrated over the bars.

To assess the impact of the parameterizations on the nearshore flow, we use the modeling suite DELFT3D (Lesser et al. 2004; Stelling 1996), with DELFT3D-FLOW and DELFT3D-WAVE running in coupled mode. For each profile, a longshore uniform 2D grid was populated with the bathymetry. The circulation was forced by a parametric wave forcing with the significant wave height $H_{sig} = 1.5$ m, peak period $T_p = 10$s, and mean wave direction θ_m oriented 10° from shore-normal. For each of the 227 Duck cases, wave heights and longshore currents were computed for the Dean and barred forms of parametric bathymetry and compared to the same quantities predicted using the true (survey) bathymetry.

Fig. 6 shows a good example of hydrodynamic results (bathymetry bias and rms errors were 0.01 and 0.22 m, respectively, at the top 95% of all fits). The longshore current (middle panel) predicted using either the Dean or composite profiles consists of a broad region of current whose peak location and width are set by the smooth underlying beach profile. Currents predicted for the true and barred profiles are much narrower and peak over the sand bar. Similarly, the wave height transects (bottom panel, Fig. 6) show a gradual decrease of wave height for the featureless profiles, in contrast with the sharp wave height decrease observed for the survey and barred beach profiles.

Several measures of performance were computed and are summarized in Table 3. For longshore currents, the bias and rms error were computed over the full domain. The average values for the barred bathymetry (−0.01 and 0.08 m/s) were significantly better than for the unbarred Dean profile (0.05 and 0.14 m/s, respectively). In addition, the cross-shore location and strength of the peak current were extracted from the full current profiles. Fig. 7 shows the predictions for the cross-shore location and strength of peak longshore currents for the surveyed, Dean, and the parametric beach profiles. Currents for the monotonic Dean profile vary only a small amount dependent on slight variations of the Dean profile fit at different longshore locations. The locations of the peak current for the barred and survey profiles are more variable, in response to the movements of the sand bar. The bias and rmse for the barred profile predictions (5.2 and 16.3 m) is much better than for the Dean profile (21.1 and 33.6 m, respectively) and the correlation of peak current position is much higher for barred bathymetry (0.85) than for the Dean bathymetry (0.12). The results for the strength of the peak current are less dramatic with the bias and rmse for barred profiles (0.05 and 0.07 m/s) lower than for the unbarred Dean profile (0.07 and 0.08 m/s) and current strength estimates improved for 62% of cases (Table 4).

Computed errors for significant wave height transects were also improved by using the barred profile (bias −0.02 m and rmse 0.11 m) compared to those found using the Dean model bathymetry (bias −0.07 and rmse 0.15 m). Errors were reduced in 82% of cases.

It should be realized that there are many cases where performance is worsened by the inclusion of parameterized sand bars. In reviewing all the results, it was found that these cases corresponded to times when

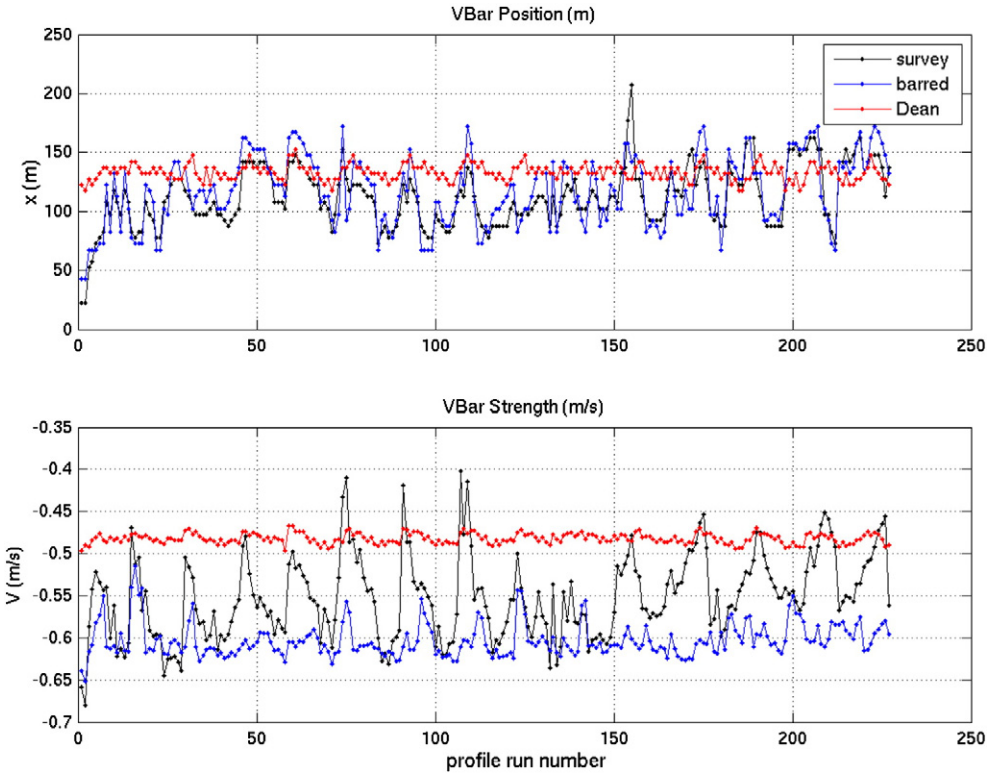

Fig. 7. Cross-shore location (upper) and strength (lower) of peak longshore current for the surveyed and parametric bathymetries.

Table 4
Comparison of hydrodynamics model results using the composite barred (middle two columns) and Dean (right two columns) profiles compared to results using surveyed data. Each comparison lists the bias and rms error. For x_{Vpeak}, the location of peak longshore current and the correlation, r, with surveyed peak current locations are also listed. Longshore current comparisons include error over the full transect (top data row) as well as the magnitude and location of the peak current, V_{peak}. The significant wave height is simply compared over the full transect.

		Barred		Dean	
		Bias (rms) (m/s or m)	r	Bias (rms) (m/s or m)	r
Longshore currents	Full transect	−0.01 (0.08)		0.05 (0.14)	
	V_{peak}	0.05 (0.07)		0.07 (0.08)	
	x_{Vpeak}	5.2 (16.3)	0.85	21.1 (33.6)	0.12
H_s		−0.02 (0.11)		0.07 (0.15)	

the sand bar was of low amplitude, poorly formed or non-existent, and so inconsistent with the climatological shape. However these occurrences were in the minority.

Comparable results for Eglin AFB are shown in Fig. 8. Again, the addition of sand bars clearly improves the hydrodynamic predictions over the monotonic composite profile (and the Dean profile, not shown). Two maxima are now seen in the longshore currents with the inner peak sharper due to the steeper inner bar profile. Current maxima are well estimated and the locations are close to those for the survey profile. Similarly, the cross-shore profile of wave height for the barred parametric beach profile is a very good approximation of that on the surveyed profile, with wave height decay concentrated in the two regions of the sand bars. By comparison, the monotonic composite profile shows only a single broad current and wave height decay curve.

Fig. 8 was based on an assumed value of h_{sea} of 8.0 m. The results were also computed for values of 6.0 and 10.0 m. Reducing h_{sea} to 6.0 m yielded little change over the inner bar but a noticeable reduction of the influence of the outer bar. In contrast, increasing h_{sea} to 10.0 m changed the deeper bathymetry but had essentially no influence on the hydrodynamics over either of the two inner sand bars where waves were breaking. This reinforces the idea that estimated parametric barred profiles will yield improved hydrodynamic predictions that are not overly sensitive to the choice of parameters.

5. Discussion

Characterization of the hydrodynamics of the nearshore domain, a common goal, requires knowledge of the underlying bathymetry, something that is expensive to measure, rapidly changing and therefore rare. However, it is not rare that we know something about model domains of interest. For instance, air photos or other remote sensing are commonly available to determine a shoreline, charts or climatological data that can be used to determine a reference offshore contour and approximate slope, while climatological foreshore slopes can reasonably be guessed from local knowledge or geology. The most dynamic part of the system is the location of submerged sand bars, features that are easy to detect using breaking wave signatures (e.g. Lippmann and Holman, 1989; van Enckevort and Ruessink, 2001). The resulting fluid models are not expected to be as accurate as those derived with perfect bathymetry, but they are shown above to provide a good approximation of the cross-shore structure of important fluid dynamics variables such as wave dissipation and wave height decay. The main error, mis-location of cross-shore dissipation and resulting flows, is forced to be small by the fact that the bar position itself is easily determined from breaking patterns forcing a correct cross-shore phase for at least the detected bar.

The value of h_{sea} is the least known parameter in the bar model. Inaccuracies in chosen value affect both the offshore extent of parametric bars and their maximum amplitude. Fortunately, both sensitivities are mostly evident at larger depths in the profile, presumably offshore of

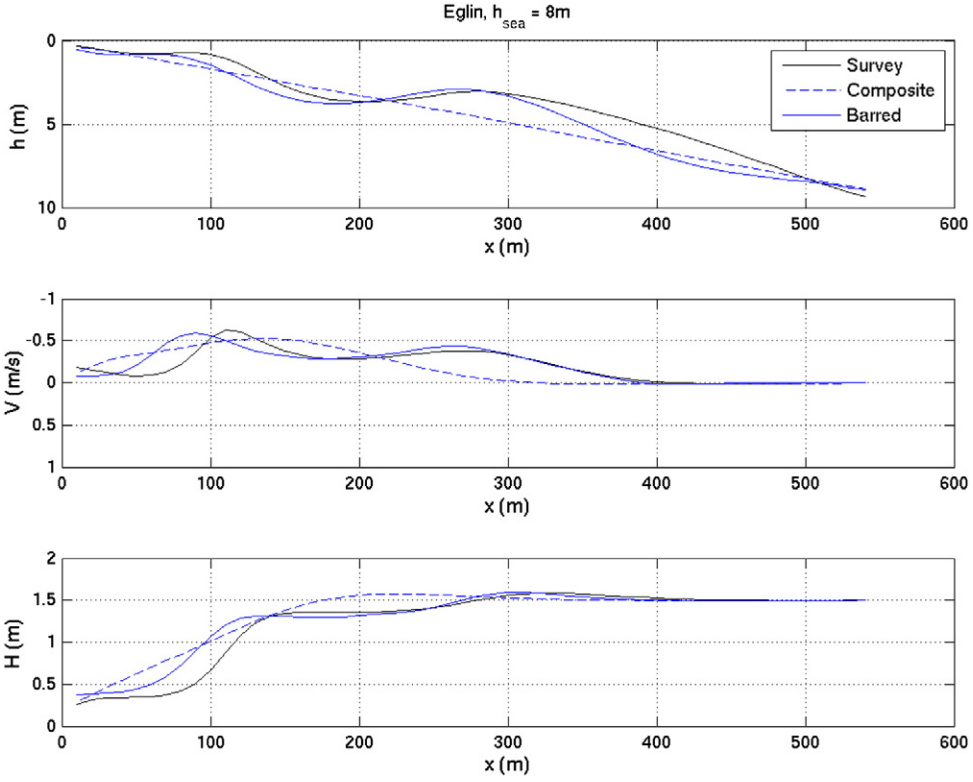

Fig. 8. Cross-shore profiles of bathymetry (upper panel), longshore current (middle panel) and significant wave height (bottom panel) computed for the true and parameterized bathymetries for Eglin AFB, assuming $h_{sea} = 8$ m. As with Duck, current and wave height decay for the barred profile is a much better approximation of truth than the broad current and slow wave height decay predicted for the unbarred parametric models.

wave breaking for non-storm waves. Thus model results are less sensitive to those bathymetry errors that they are to surf zone bathymetry errors.

The current method is limited to 1DH profiles so does not represent 2DH bathymetry directly. However, a 2DH morphology could potentially be represented by an integrated set of adjacent 1DH slices. The potential success of this method would need further investigation.

Finally, it bears repeating that the parameterized profile proposed by Dean makes no pretense of representing sand bars, so the comparisons and discussion made here should not be interpreted as criticism of the Dean profile for longer term climate change and coastal response purposes.

6. Conclusions

A method is proposed and tested for estimating equilibrium bathymetric profiles that include realistic sand bars superimposed on a concave up background form. The bar function, taken from Ruessink et al. (2003b), has a cosine form with spatially variable amplitude and wavelength whose characteristics are a function of the background profile (long-term average depth) and a climatological estimate of the maximum depth of the sand bar activity. The cross-shore locations of all bars and troughs are determined by a single phase that can readily be estimated by almost any remote sensing modality. Previous literature forms for the background equilibrium profile are extended with a new composite form that blends an exponential nearshore concave up surface with an asymptotic planar slope offshore, beyond the effects of wave action. Aside from the cross-shore phase, the profiles depend on four other parameters, all of which can be estimated from climatology or approximate offshore chart data.

The parametric profiles are compared to survey bathymetry at three locations. For the 253 measured profiles from Duck, NC, bias and rms error were reduced in about 80% of the cases by using the barred parametric form compared to a standard monotonic equilibrium form. The results were similar in tests at several Pacific Coast and one Gulf of Mexico beaches. For cases for which the error statistics were not improved, the predicted profiles often looked very similar to surveys but with bars that were spatially misplaced at some locations, presumably due to the transient (non-equilibrium) nature of the bar system at that location and time. Nevertheless, the proper representation of bar-scale features is required to allow realistic predictions of nearshore hydrodynamics. Comparisons of predicted hydrodynamics using Delft3D on the surveyed, barred and monotonic equilibrium profiles show that the peak strength and cross-shore profile of longshore currents as well the decay profile of wave height are much better predicted using barred parametric versus monotonic equilibrium profile forms.

Acknowledgments

The work was supported by the Office of Naval Research through the 6.2 NRL Rapid Transition Project “Coastal Surge and Inundation Prediction System”, Program Element #0602435N.

References

Birkemeier, W.A., Mason, C., 1984. The CRAB: a unique nearshore surveying vehicle. J. Surv. Eng. 110, 1–7.
Bodge, K.R., 1992. Representing equilibrium beach profiles with an exponential expression. J. Coast. Res. 8 (1), 47–55.
Bowen, A.J., 1980. Simple models of nearshore sedimentation; beach profiles and longshore bars. In: McCann, S.B. (Ed.), The Coastline of Canada. Geological Survey of Canada, pp. 1–11.
Bruun, P., 1954. Coast erosion and the development of beach profiles: technical memorandum Rep.
Dean, R.G., 1987. Coastal Sediment Processes: Toward Engineering Solutions, Paper Presented at Proceedings of the Specialty Conference on Coastal Sediments, ASCE.
Dean, R.G., 1991. Equilibrium beach profiles: characteristics and applications. J. Coast. Res. 7, 53–84.
Komar, P.D., McDougal, W.G., 1994. The analysis of beach profiles and nearshore processes using the exponential beach profile form. J. Coast. Res. 10 (59–69).
Larson, M., Kraus, N.C., 1989. SBEACH: numerical model to simulate storm-induced beach change Rep.
Lippmann, T.C., Holman, R.A., 1989. Quantification of sand bar morphology: a video technique based on wave dissipation. J. Geophys. Res. 94 (C1), 995–1011.
Ozkan-Haller, H.T., Brundidge, S., 2007. Equilibrium beach prfile concept for Delaware Beaches. J. Waterw. Port Coast. Ocean Eng. 133 (2), 147–160. http://dx.doi.org/10.1061/(ASCE)0733-950X.
Plant, N.G., Holman, R.A., Freilich, M.H., 1999. A simple model for interannual sand bar behavior. J. Geophys. Res. 104 (C7), 15755–15776.
Plant, N.G., Freilich, M.H., Holman, R.A., 2001. The role of morphological feedback in surf zone sand bar response. J. Geophys. Res. 106 (C1), 973–989.
Ruessink, B.G., Walstra, D.J.R., Southgate, H.N., 2003a. Calibration and verification of a parametric wave model on barred beaches. Coast. Eng. 48, 139–149.
Ruessink, B.G., Wijnberg, K.M., Holman, R.A., Kuriyama, Y., van Enckevort, I.M.J., 2003b. Inter-site comparisons of interannual nearshore bar behavior. J. Geophys. Res. 108. http://dx.doi.org/10.1029/2002JC001505.
Ruggiero, P., Kaminsky, G.M., Gelfenbaum, G., Voigt, B., 2005. Seasonal to interannual morphodynamics along a high-energy dissipative littoral cell. J. Coast. Res. 21 (3), 553–578.
Ruggiero, P., Eshleman, J.L., Kingsley, E., Thompson, D.M., Voigt, B., Kaminsky, G.M., Gelfenbaum, G., 2007. Beach Morphology Monitoring in the Columbia River Littoral Cell: 1997-2005 Rep.
van Enckevort, I.M.J., Ruessink, B.G., 2001. Effect of hydrodynamics and bathymetry of video estimates of nearshore sand bar position. J. Geophys. Res. 106 (C8) (16969-916979).